

Analysis of effects of Young modulus variations on Brillouin power and Brillouin frequency shift changes in optical fibers

ABDURRAHMAN GÜNDAY^a, SAİT ESER KARLIK^{b*}, GÜNEŞ YILMAZ^b

^a*Program of Electronics Technology, Vocational School of Orhangazi, Uludağ University, 16800 Orhangazi, Bursa, Turkey*

^b*Department of Electrical & Electronics Engineering, Faculty of Engineering, Uludağ University, 16059 Görükle, Bursa, Turkey*

Brillouin scattering mechanism and Young modulus variations in optical fiber distributed sensing systems are directly affected by ambient temperature and thermal strain formations. Generally, in such sensing systems where temperature and strain formations are detected and measured simultaneously, Brillouin frequency shift and Brillouin power changes of backscattered optical signal are used due to their temperature and strain dependencies. In this research, a different point of view has been developed and effects of Young modulus variations of the sensing fiber core on the Brillouin power and the Brillouin frequency shift changes have been analyzed. In this study, positioning five heating units at different locations along a 1000 m G.652 type single-mode fiber operating at 1550 nm, a sensing system model has been constructed. On this model, simulations related to Young modulus variations along the sensing fiber depending on temperature fluctuations generated by heating units have been performed using Matlab 2010 and results have been obtained for 1000 different points with a spatial resolution of 1 m. For 40 °C - 47 °C operating temperature range of the sensing fiber, the Young modulus of the fiber core changes from 73.205 GPa to 73.283 GPa. Furthermore, using the analytical method, linear formula between the Young modulus and Brillouin parameters, i.e. Brillouin power and Brillouin frequency shift changes, of the backscattered optical signal have been derived. Thus, for the system model constructed, Matlab simulations analyzing relations between Young modulus variations and Brillouin parameter changes have been performed under specified operating conditions. For Young modulus variations in 73.205 GPa - 73.283 GPa range, values of Brillouin power and Brillouin frequency shift changes have been obtained in ranges of 13.950 % - 16.273 % and 69.00 MHz - 85.72 MHz, respectively. Moreover, temperature and thermal strain resolutions along the sensing fiber have been acquired as ~ 0.7 °C and ~ 40 µε, respectively.

(Received April 19, 2016; accepted November 25, 2016)

Keywords: Optical fiber distributed sensing, Brillouin power change, Brillouin frequency shift change, Young modulus, Temperature, Thermal strain

1. Introduction

Optical fibers are widely used in sensing systems to detect various parameters [1-7]. Optical fiber distributed sensing systems, which are based on Rayleigh, Raman and Brillouin scattering mechanisms and working principles, can detect temperature, strain and pressure information from any point along the sensing fiber with high resolution and accuracy.

Furthermore, Brillouin scattering based optical fiber distributed sensing systems have gained much interest due to their potential opportunities for measuring and detecting temperature and strain variations simultaneously. Especially they are widely used for monitoring temperature and strain variations not only in underground, overhead and submarine power cables, but also in aerospace and oil industries and civil engineering structures such as bridges, tunnels, large buildings, etc. [3, 6]. In these systems, using Brillouin frequency shift change and Brillouin power change information of the backscattered optical signal in the sensing fiber, required data related to the ambient thermal characteristics can be

easily reached. Since Young modulus of the silica fiber core has both temperature and strain dependencies [8], in order to detect these two parameters along the sensing fiber, Young modulus changes can be used as well [9].

In this study, effects of Young modulus variations on Brillouin power change and Brillouin frequency shift change have been theoretically analyzed and using results of this theoretical analysis, simulations have been performed along the sensing fiber of the distributed sensing system model prepared.

In principle, Brillouin scattering based distributed sensing systems are founded on the interaction of photons pumped by the laser source inside the sensing fiber with thermally generated acoustic waves and detection of the backscattered optical signal by APD (avalanche photodiode). This kind of sensing system uses the BOTDR (Brillouin optical time domain reflectometry) monitoring technique [1, 10, 11].

In BOTDR, the light is launched into one end of the sensing fiber by a laser source and the light partially backscattered is detected at the same end of the fiber. In other words, in this technique, only one end of the sensing

fiber is used while the other end of the fiber is generally terminated. Using the BOTDR technique, temperature and thermal strain profiles along the sensing fiber are obtained from Brillouin frequency shift change and Brillouin power change making use of their temperature and thermal strain dependencies [1, 10, 12].

A schematic diagram of the optical fiber distributed temperature sensing (DTS) and distributed thermal strain sensing (DTSS) system based on Brillouin scattering mechanism is shown in Fig. 1 [10]. This system used for simultaneous sensing of temperature and thermal strain profiles through the optical fiber has been utilized as the model for simulations performed in this study. In this model, optical pulses produced by a laser source are amplified using Erbium doped fiber amplifier EDFA1 and are then pumped into the sensing fiber via the acousto-optic modulator AOM1. Circulator C1 is used for directing the optical signal amplified by EDFA2 to heating units located on specific regions of the sensing fiber. In those regions of the sensing fiber, thermal formations generated by heating units cause the backscattered optical signal including Rayleigh (R), Brillouin Stokes (BS) and Brillouin anti-Stokes (BAS) components routing back to the circulator C1. In the model, the weak backscattered optical signal routed towards the circulator C1 is amplified by EDFA3 and then directed to the sensing system.

When the backscattered optical signal is amplified by EDFA3, ASE (amplified spontaneous emission) noise can exist in the sensing system. Therefore acousto-optic modulator AOM2 is added to the output end of amplifier to suppress the ASE noise and modulate the signal via acousto-optic effect. A 95/5 directional coupler placed in the sensing model has two arms one of which is linked to the pulse monitor (PM) unit. In order to get information about the system output power, 5 % of the backscattered signal is monitored by the PM unit. The other arm of the directional coupler is used to detect Rayleigh backscattered optical signal utilized for normalizing Brillouin backscattered signal power traces [10].

Circulator C2 is added to the sensing model to route the backscattering signal including Rayleigh and Brillouin components towards the Fiber Bragg Grating (FBG). FBG is used to reflect the optical signal at a specific wavelength (λ_B) and to transmit optical signals at all other wavelengths in the spectrum. Furthermore, since the Brillouin backscattering signal is approximately 10^5 times weaker than the signal pumped, usage of FBG in the model is important in filtering the Brillouin anti-Stokes component from the Rayleigh signal. In this model, FBG reflects backscattering Brillouin anti-Stokes (BAS) components towards C2, while it transmits backscattering Brillouin Stokes (BS) and Rayleigh (R) components. Then Brillouin anti-Stokes component arrives back to the circulator C2 and is routed by the circulator to the sensing unit. The optical local oscillator (LO) signal transmitted via FBG positioned at the output of the 50/50 directional coupler is then mixed with the Brillouin anti-Stokes signal. Thus, a beat frequency with a value of ~ 11.50 GHz is generated and it is detected by a photodetector sensitive to this frequency value in the sensing unit [10].

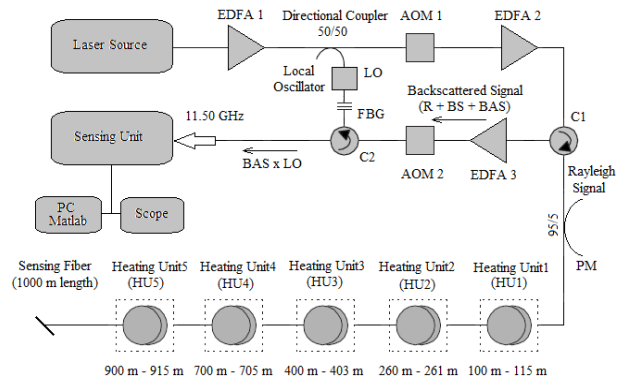


Fig. 1. Distributed temperature sensing (DTS) and distributed thermal strain sensing (DTSS) system

The sensing system is used to detect time-domain traces at a specific radio frequency (RF) band. For a frequency value detected by the photodetector, the Brillouin spectrum along the sensing fiber can be determined with time-domain traces.

Finally, Brillouin frequency shift change and Brillouin power change information, i.e. Brillouin parameters, along the sensing fiber can be obtained with computational methods performed by a PC located at the output of the sensing unit. Making use of those Brillouin parameters, temperature and thermal strain formations along the fiber can also be monitored. Using distributed sensing systems based on the combined effect of the Brillouin scattering and the Young modulus change and benefiting from their temperature and thermal strain dependencies, variations in the Young modulus, the Brillouin power and Brillouin frequency shift changes can be possibly detected and measured at high resolutions.

2. Temperature and strain dependencies of Brillouin power and Brillouin frequency shift changes

Assuming that powers of the optical signal propagating at forward direction along the fiber and the backscattering signal are equal, the Brillouin signal power backscattered along the fiber can be given as a function of time t as in [8]

$$P_B(t) = 0.5P_0\tau\gamma_B S v_g e^{(-\gamma_R v_g t)} \quad (1.a)$$

where P_0 is the peak power of the laser pumping signal, τ is the pulse duration, γ_B and γ_R are the Brillouin and Rayleigh backscattering coefficients, respectively, S is the capturing coefficient, v_g is the group velocity of light propagating in the fiber and t is the time [10, 13].

Making use of the equation $t = 2z/v_g$, Brillouin power P_B can be obtained as a function of distance z as in [10, 13]

$$P_B(z) = 0.5P_0\tau\gamma_B S v_g e^{(-2\gamma_R z)} \quad (1.b)$$

Although the Brillouin backscattering coefficient γ_B of (1.b) has a direct dependence to ambient temperature variations, the Rayleigh backscattering coefficient γ_R does not have such a direct dependence [8]. Therefore, effects of temperature variations on the Brillouin signal power occur via γ_B which can be written as [10, 13]

$$\gamma_B = \frac{8\pi^3 n^8 p^2 k T (\rho v_a^2)^{-1}}{3\lambda_0^4} \quad (2)$$

where n is the fiber core refractive index, p is the photoelastic (Pockel) coefficient (~ 0.286), k is the Boltzmann's constant (1.38×10^{-23} J/°K), T is the fiber temperature in terms of °K, ρ is the density of the silica fiber ($\rho = 2330$ kg/m³), v_a is the acoustic wave velocity in glass and λ_0 is the wavelength of light launched into the fiber ($\lambda_0 = 1550$ nm) [10, 13].

In Brillouin scattering mechanism, the optical wave pumped by the laser source into the fiber interacts with thermally generated acoustic waves in the medium and hence it is scattered with an angle θ [10]. Thermally generated acoustic waves have a broadband frequency spectrum. When the optical wave pumped into the fiber is phase-matching with the acoustic wave, i.e. when the Bragg condition occurs, the Brillouin frequency shift occurs at a specific value. This value is equal to the frequency of the acoustic wave f_a .

The acoustic frequency f_a satisfying the Bragg condition can be described as [10]

$$f_a = \frac{2n}{\lambda_0} v_a \sin \frac{\theta}{2} \quad (3)$$

where θ is the angle between the optical wave pumped into the fiber and the Brillouin scattered wave.

In optical fibers, the scattered optical wave is guided only in either forward or backward directions. If the optical wave is scattered in the opposite direction of the pumped wave, i.e. when $\theta = 180^\circ$, the acoustic frequency f_a is maximized. Thus, since the Brillouin frequency shift V_B is equal to the acoustic frequency f_a , then one can write [3, 10, 14, 15]

$$V_B = \frac{2n}{\lambda_0} v_a \quad (4)$$

Since Brillouin power P_B and Brillouin frequency shift V_B change with temperature and strain variations, equations describing temperature and strain dependencies of Brillouin power change (ΔP_B) and Brillouin frequency shift change (ΔV_B) can be given as [10, 14, 15]

$$\Delta P_B = K_T^P \Delta T + K_\epsilon^P \Delta \epsilon \quad (5)$$

$$\Delta V_B = K_T^V \Delta T + K_\epsilon^V \Delta \epsilon \quad (6)$$

where K_T^P and K_ϵ^P are the temperature and strain coefficients of the Brillouin power change, respectively,

K_T^V and K_ϵ^V are the temperature and strain coefficients of the Brillouin frequency shift change, respectively, ΔT and $\Delta \epsilon$ are temperature and strain changes occurring along the sensing fiber, respectively.

Temperature and strain coefficients of Brillouin parameters for G.652 type single mode fiber (SMF) are given in Table 1 [10].

Table 1. Temperature and strain coefficients for G.652 SMF

Coefficients	Values
K_T^P	0.36 ± 0.030 %/(°C)
K_ϵ^P	$-9 \times 10^{-4} \pm 1 \times 10^{-5}$ %/($\mu\epsilon$)
K_T^V	1.07 ± 0.06 MHz/(°C)
K_ϵ^V	0.048 ± 0.004 MHz/($\mu\epsilon$)

The sensing performance of distributed optical fiber sensing systems is evaluated with the help of temperature and thermal strain resolutions. Related resolutions for temperature and thermal strain formations occurring along the sensing fiber can be computed with [10]

$$\delta_T = \frac{[K_\epsilon^P \delta V] + [K_\epsilon^V \delta P]}{[K_\epsilon^V K_T^P - K_\epsilon^P K_T^V]} \quad (7)$$

$$\delta_\epsilon = \frac{[K_T^P \delta V] + [K_T^V \delta P]}{[K_\epsilon^V K_T^P - K_\epsilon^P K_T^V]} \quad (8)$$

where δ_T and δ_ϵ are temperature and thermal strain resolutions, respectively, δP and δV are RMS noise values occurring on the Brillouin power change and the Brillouin frequency shift change, respectively.

3. Young modulus dependencies of Brillouin power and Brillouin frequency shift changes

Young modulus is one of the fundamental criteria used for describing elastic properties of a material. When an external force is applied onto an object, depending on the material characteristics, the object is exposed to longitudinal and lateral elongations that create uniaxial stress and strain variations on the material of the object according to the Hooke's Law [16]. Young modulus, i.e. the elasticity modulus, is defined as the ratio of the stress variation at any point on the material to the strain variation at that point as [16, 17, 18]

$$E = \frac{\sigma}{\epsilon} = \frac{F/S}{\Delta L/L} \quad (9)$$

where σ denotes the tensile stress and ϵ denotes the tensile strain occurred on the object, F is the force acting on the object, S is the cross-sectional area where the force is acting on, ΔL is the amount of variation in length and L is the original length of the object.

The Young modulus of fused silica fiber varies linearly with ambient temperature and the thermal strain formations in the medium. Temperature and thermal strain

dependencies of the Young modulus of the silica fiber core can be given as

$$E = 69.68 + 1.126 \times 10^{-2}T \quad (10)$$

$$E = E_0(1 + 5.75 \times \epsilon) \quad (11)$$

respectively [8, 13], where E is the Young modulus of the fiber core in terms of GPa, E_0 is the value of the Young modulus at zero strain and 293 °K temperature, i.e. $E_0 = 72.97918$ GPa, T is the temperature in terms of °K, ϵ is the strain.

Using (10) and (11), temperature formations T_K and thermal strain formations ϵ occurred along the sensing fiber can be obtained as a function of the Young modulus of the fiber core as given in (12) and (13), respectively,

$$T_K = 88.81 \times E - 6188.277 \quad (12)$$

$$\epsilon = 2383.05 \times E - 1.739 \times 10^5 \quad (13)$$

Converting the temperature term from °K to °C, (12) takes the form in (14)

$$T_C = 88.81 \times E - 6461.277 \quad (14)$$

where T_C is the temperature formations along the sensing fiber length in terms of °C.

Using (5) and (6), Brillouin power change ΔP_B and Brillouin frequency shift change ΔV_B can be written as in (15) and (16), respectively

$$\Delta P_B = K_T^P \Delta T_C + K_\epsilon^P \Delta \epsilon \quad (15)$$

$$\Delta V_B = K_T^V \Delta T_C + K_\epsilon^V \Delta \epsilon \quad (16)$$

where ΔT_C and $\Delta \epsilon$ are temperature and strain changes occurring along the sensing fiber, respectively.

Generalizing (5) and (6), the Brillouin power change and the Brillouin frequency shift change along the sensing fiber can be obtained as

$$\Delta P_B(L) = K_T^P T_C(L) + K_\epsilon^P \epsilon(L) \quad (17)$$

$$\Delta V_B(L) = K_T^V T_C(L) + K_\epsilon^V \epsilon(L) \quad (18)$$

Using (13), (14) and temperature and strain coefficients given in Table 1 in (17) and (18) and reorganizing the equations, the Brillouin power change and the Brillouin frequency shift change can be written as a function of the Young modulus as

$$\Delta P_B(E) = 29.827 \times E - 2169.550 \quad (19)$$

$$\Delta V_B(E) = 209.413 \times E - 15260.766 \quad (20)$$

respectively, where E is the Young modulus of the sensing fiber core in GPa. As it is obvious in equations, there is a linear relation between the Young modulus and the Brillouin power change and the Brillouin frequency shift

change of the backscattered optical signal guided along the sensing fiber.

Since Young modulus of the fiber core varies with ambient temperature and strain formations, effects of Young modulus changes on Brillouin parameters are very important in terms of the sensing system performance. Therefore, for different Young modulus values of the fiber core, different Brillouin power change and Brillouin frequency shift change data can be obtained at the output of the sensing system.

Young modulus sensitivities of the Brillouin power change and the Brillouin frequency shift change can be given as

$$\frac{d\Delta P_B(E)}{dE} / \Delta P_B(E) = \frac{29.827}{29.827 \times E - 2169.550} \quad (21)$$

$$\frac{d\Delta V_B(E)}{dE} / \Delta V_B(E) = \frac{209.413}{209.413 \times E - 15260.766} \quad (22)$$

respectively.

Using (21) and (22), the ratio of the Young modulus sensitivity of the Brillouin frequency shift change to that of the Brillouin power change for zero strain and 293 °K temperature can be computed as ~ 2.30 . Therefore, it can be concluded that the Young modulus has a more dominant effect on the Brillouin frequency shift change with respect to the Brillouin power change.

4. Simulations

Simulations have been performed using Matlab 2010 on the simulation model built up for analyzing effects of Young modulus changes on the Brillouin power change and the Brillouin frequency shift change.

Table 2. Locations of heating units along the sensing fiber

Heating Units	Locations
HU1	100 m – 115 m
HU2	260 m – 261 m
HU3	400 m – 403 m
HU4	700 m – 705 m
HU5	900 m – 915 m

In this research, heating effects on the sensing fiber have been modeled by positioning five heating units at different locations along the cable. In similar papers presented in the literature, thermal formations occurring along the sensing fiber have been modeled with heating units such as ovens [8, 10] and lamps [19]. Locations of heating units positioned along the sensing fiber in the model are given in Table 2.

Parameters of the sensing fiber and the laser source used in the model for simulations are given as follows: Pulse duration of the optical signal pumped by the laser (τ) is 10 ns, maximum power of the optical signal pumped by

the laser (P_0) is 1.5 W, wavelength of the optical signal pumped into the sensing fiber (λ) is 1550 nm, refractive indices of the optical fiber core and cladding (n_1 and n_2) are 1.50 and 1.45, respectively, fiber attenuation coefficient at 1550 nm (γ) is $4.56 \times 10^{-5} \text{ m}^{-1}$, speed of the light in vacuum (c) is $3 \times 10^8 \text{ m/s}$, acoustic velocity in the glass (v_a) is 5960 m/s, group velocity of the light propagating in the fiber ($v_g = c/n_1$) is $2 \times 10^8 \text{ m/s}$, spatial resolution ($l = c\tau/2n_1$) is 1.0 m, length of the fiber cable (L) is 1000 m, number of measurement points for DTS ($R = L/l$) is 1000, density of the silica fiber (ρ) is 2330 kg/m^3 and capturing coefficient ($S = (n_1^2 - n_2^2)/4n_1^2$) is 16.389×10^{-3} .

Temperature variation along the sensing fiber is shown in Fig. 2.

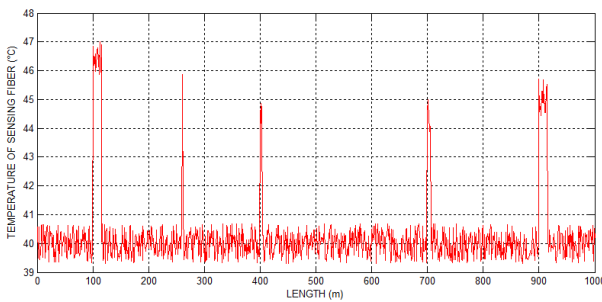


Fig. 2. Temperature variation along the sensing fiber

As it is obvious in Fig. 2, heating effects of HUs used in the model create hot points. The sensing fiber reaches to its highest temperature value while passing through the heating unit HU1 between 100th meter and 115th meter since the heating unit HU1 has higher heating power than other heating units. In this region of the fiber, average temperature value is $\sim 46.50 \text{ }^\circ\text{C}$ and the maximum value is $47 \text{ }^\circ\text{C}$ at the 113th meter.

Using (10), the simulation result obtained for variation of the Young modulus of the sensing fiber core with varying ambient temperature is shown in Fig. 3. Except the five regions where the sensing fiber is passing through heating units, the Young modulus of the fiber core along the sensing fiber takes a value of 73.205 GPa for the average temperature value of $40 \text{ }^\circ\text{C}$ (313 K). Young modulus variation of the fiber due to the variation of the ambient temperature reaches to its maximum value with 73.283 GPa at the 113th meter of the sensing fiber. As it is obvious in Fig. 3 that temperature dependence of the Young modulus of the fiber core is $\sim 11 \text{ MPa/}^\circ\text{K}$ in the temperature range of $313 \text{ K} - 320 \text{ K}$.

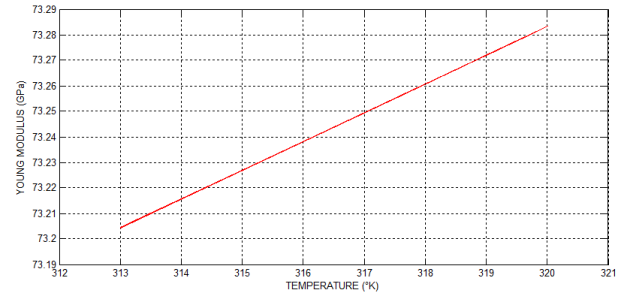
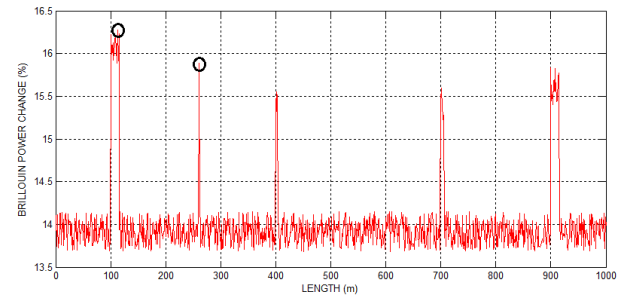
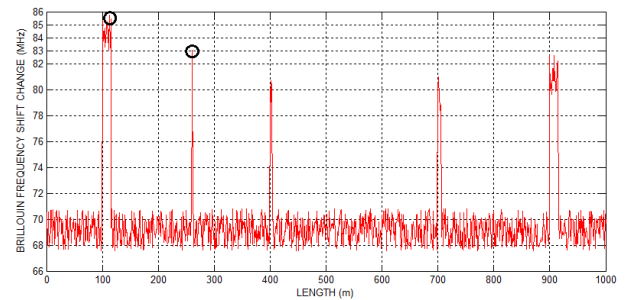


Fig. 3. Variation of the Young modulus of the sensing fiber core with varying ambient temperature

The Brillouin power change and the Brillouin frequency shift change occurring along the sensing fiber are shown in Fig. 4.



(a)



(b)

Fig. 4. a) The Brillouin power change and b) the Brillouin frequency shift change along the sensing fiber

As it is obvious, the Brillouin power change of the backscattered optical signal reaches to its maximum values as a result of temperature increments at hot points created by HUs. As it can be easily seen that the highest peak of the Brillouin power change is again at the 113th meter with 16.273 % where the Young modulus also reaches to its maximum value. In the second region of the sensing fiber where it is passing through the heating unit HU2, the Brillouin power change takes the value of 15.887 %. The Brillouin frequency shift change gets its maximum two values of 85.720 MHz and 83.012 MHz on the first two hot spot regions of the sensing fiber, respectively, as shown in Fig. 4b.

Using the simulation results given in Fig. 4, RMS noise values occurring on the Brillouin power change and the Brillouin frequency shift change have been determined as $\delta P = 0.225\%$ and $\delta V = 1.40$ MHz, respectively. Substituting δP and δV values as well as values of coefficients given in Table 1 in (7) and (8), temperature and thermal strain resolutions along the sensing fiber have been computed as ~ 0.7 °C and ~ 40 $\mu\epsilon$, respectively.

Using (19) and (20), simulation results obtained for variations of the Brillouin parameters with varying Young modulus of the sensing fiber are shown in Figs. 5a and 5b, respectively.

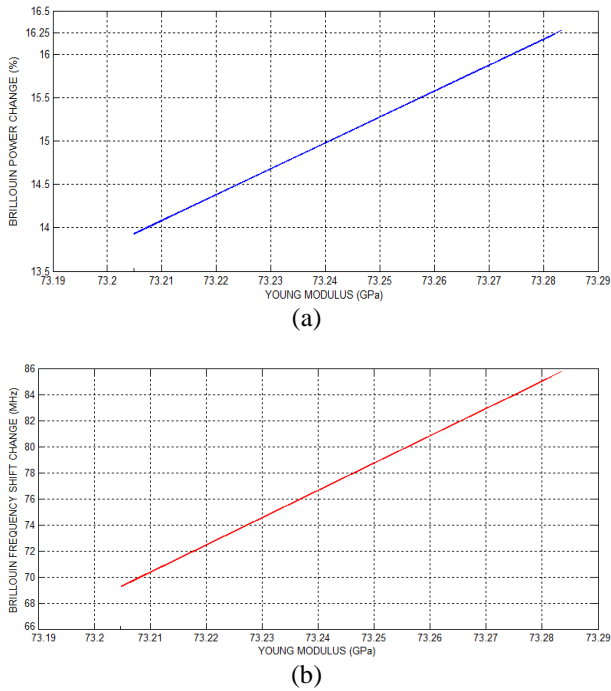


Fig. 5. a) Variation of the Brillouin power change and b) variation of the Brillouin frequency shift change with varying Young modulus of the sensing fiber core

As it is obvious in Fig. 5, the Brillouin power change and the Brillouin frequency shift change are linearly affected by variations of the Young modulus of the sensing fiber core. Consequently, values of the Brillouin power change and the Brillouin frequency shift change increase with increasing values of the Young modulus of the fiber core, otherwise they decrease with decreasing values of the Young modulus. According to simulation results, Young modulus dependencies of the Brillouin power change and the Brillouin frequency shift change have been computed as 30 %/GPa and 210 MHz/GPa, respectively.

In regions where sensing fiber is passing through heating units, average values of the Brillouin power change, the Brillouin frequency shift change and the Young modulus of the fiber core are given in Table 3.

Table 3. Average values of Brillouin parameters and Young modulus variations at hot spot regions along the sensing fiber

Region of the Sensing Fiber	Young Modulus (GPa)	Brillouin Power Change (%)	Brillouin Frequency Shift Change (MHz)
100 m – 115 m	73.277	16.08	84.60
260 m – 261 m	73.270	15.87	82.92
400 m – 403 m	73.255	15.43	79.78
700 m – 705 m	73.260	15.58	80.83
900 m – 915 m	73.262	15.64	81.25

All values given in Table 3 for the Brillouin power change, the Brillouin frequency shift change and the Young modulus have been computed by averaging values of the related parameter obtained from all measurement points of the considered region. For example, in 100 m - 115 m region of the sensing fiber, taking 1.0 m spatial resolution into account, there are 16 measurement points. Therefore related values in Table 3 show the arithmetical means of parameters obtained in those 16 points.

Using (21) and (22), for Young modulus given in Table 3 the Young modulus sensitivity of the Brillouin frequency shift change can be computed as ~ 1.35 times greater than that of the Brillouin power change.

5. Conclusion

In this study, making use of the optical fiber distributed sensing method based on the combined effect of Brillouin scattering and Young modulus change of the fiber core, relations between Brillouin parameters and the Young modulus have been analyzed theoretically and simulations related to these analyses have also been performed.

For temperature variations of the sensing fiber in the range of 40 °C - 47 °C, the Brillouin power change and the Brillouin frequency shift change of the backscattered optical signal vary in the range of 13.950 % - 16.273 % and 69.00 MHz - 85.72 MHz, respectively. Therefore, a 1 °C variation in the temperature of the fiber core causes a 0.3319 % variation on the Brillouin power change and a 2.3886 MHz variation on the Brillouin frequency shift change. Simulation results show that the Young modulus sensitivity of the Brillouin frequency shift change is ~ 1.35 times greater than that of the Brillouin power change for hot spot regions. Temperature and thermal strain resolutions along the sensing fiber have been obtained as ~ 0.7 °C and ~ 40 $\mu\epsilon$, respectively. These are promising values for highly-accurate sensing of thermal formations occurring along power cables covering ultra-long distances.

It can be possible to make modifications on the Young modulus of the fiber core by doping, changing the refractive index of the fiber core or its density during the

production of the optical fiber cable. Modifying the Young modulus of the fiber core with supports of additional processes stated above, it is possible to make variations on values of the Brillouin power change and the Brillouin frequency shift change along the sensing fiber if desired. Thus, sensitivities and performances of optical fiber distributed sensing systems can be improved.

Furthermore, this study forms a background for future investigations and projects related to optical fiber distributed sensing systems using variations of the Young modulus and Brillouin parameters simultaneously in the detection process.

References

- [1] X. Bao, L. Chen, *Sensors*, **12**, 8601 (2012).
- [2] S. W. Harun, M. Yasin, A. Hamzah, H. Ahmad, *J. Optoelectron. Adv. M.* **13**(1), 69 (2011).
- [3] A. Minardo, R. Bernini, L. Amato, L. Zeni, *IEEE Sensors J.* **12**(1), 145 (2012).
- [4] A. Lokman, N. Irawati, H. Arof, S. W. Harun, N. M. Ali, *Optoelectron. Adv. Mat.* **8**(5-6), 395 (2014).
- [5] M. Yasin, S. W. Harun, H. Ahmad, *J. Optoelectron. Adv. M.* **13**(8), 933 (2011).
- [6] H. S. Pradhan, P. K. Sahu, *Optik* **125**(1), 441 (2014).
- [7] D. Sengupta, M. Sai Shankar, P. Saidi Reddy, R. L. N. Sai Prasad, K. Srimannarayana, *Optoelectron. Adv. Mat.* **4**(12), 1933 (2010).
- [8] K. R. C. P. De Souza, *Fiber optic distributed sensing based on spontaneous Brillouin scattering*, PhD Dissertation, University of Southampton (1999).
- [9] A. Gunday, S. E. Karlık, G. Yilmaz, *Journal of the Faculty of Engineering and Architecture of Gazi University*, **29**(3), 517 (2014).
- [10] M. Alahbabi, *Distributed optical fiber sensors based on the coherent detection of spontaneous Brillouin scattering*, PhD Dissertation, University of Southampton (2005).
- [11] J. Geng, S. Staines, M. Blake, S. Jiang, *Appl. Opt.* **46**(23), 5928 (2007).
- [12] L. Zhao, Y. Li, Z. Xu, Z. Yang, A. Lü, *Sensors and Actuators A: Physical*, **216**, 28 (2014).
- [13] A. Gunday, S. E. Karlık, G. Yilmaz, *International Review of Electrical Engineering (IREE)*, **8**(2), 920 (2013).
- [14] S. M. Maughan, H. H. Kee, T. P. Newson, *Meas. Sci. Technol.* **12**(7), 834 (2001).
- [15] T. R. Parker, M. Farhadiroushan, R. Feced, V. A. Handerek, A. J. Rogers, *IEEE J. Quantum Electron.* **34**(4), 645 (1998).
- [16] T. Wiecek, *Composites Part A: Appl. Sci. and Manufacturing*, **60**, 1 (2014).
- [17] K. Onaran, *Malzeme Bilimi (Material Science) 11th Edition*, Bilim Teknik Publishing House, İstanbul, (in Turkish) (2009).
- [18] W. H. Wang, *Progress in Materials Science*, **57**(3), 487 (2012).
- [19] M. Cirigliano, G. Cattaneo, P. Boffi, A. Barberis, U. Perini, G. Pirovano, M. Martinelli, *Proc. SPIE 7503 20-th Intern. Conf. on Optical Fiber Sensors*, Edinburgh, UK, 2009, p. 75034P-1.

*Corresponding author: ekarlik@uludag.edu.tr